International Journal of Pharmaceutics 415 (2011) 232–243

Contents lists available at ScienceDirect

International Journal of Pharmaceutics

journal homepage: www.elsevier.com/locate/ijpharm

Pharmaceutical Nanotechnology

Nanostructured lipid carrier versus solid lipid nanoparticles of simvastatin: Comparative analysis of characteristics, pharmacokinetics and tissue uptake

Radheshyam Tiwari, Kamla Pathak*

Department of Pharmaceutics, Rajiv Academy for Pharmacy, Mathura, Uttar Pradesh 281001, India

ARTICLE INFO

Article history:
Received 12 February 2011
Received in revised form 16 May 2011
Accepted 18 May 2011
Available online 26 May 2011

Keywords:
Simvastatin
Nanostructured lipid carriers
Factorial design
In vitro drug release
In vitro–in vivo correlation

ABSTRACT

Nanostructured lipid carrier (NLC) system of simvastatin was investigated for improvement in release, pharmacokinetics and biodistribution over its solid lipid nanoparticles (SLN). The NLC formulations prepared by solvent injection technique were optimized by 2^3 full factorial design. Optimized NLC was deduced on the basis of dependent variables that were analyzed using Design expert 8.0.2® software (Stat Ease, Inc., USA). Pareto charts and response surface plots were utilized to study the effect of variables on the response parameters. The optimized NLC was a suspension of nanosized homogeneous particles with significantly higher entrapment efficiency (>90%) and lower recrystallization properties ($p < 0.01$) than SLNs. The pharmacokinetic parameters of Tc^{99} labeled optimized NLC in mice, obtained using Quickcal software (Plexus, India) revealed 4.8 folds increase in bioavailability as compared to simvastatin suspension and 2.29 folds as compared to SLNs. Biodistribution study revealed preferential accumulation of NLC in the liver and this is advantageous because liver is the target organ for simvastatin. IVIVC studies demonstrated level A correlation between *in vitro* release and percent drug absorbed. This investigation demonstrated the superiority of NLC over SLN for improved oral delivery and it was deduced that the liquid lipid, oleic acid was the principal formulation factor responsible for the improvement in characteristics, pharmacokinetics and biodistribution of NLCs.

1. Introduction

Attention is being focused on nanotechnology-based drug delivery systems including biodegradable polymeric nanoparticles, smart polymeric micelles, nanocrystals, nanosuspension, nanoemulsions and lipid nanoparticles with the aim to improve low aqueous solubility or oral bioavailability to bring about satisfactory therapeutic efficacy. Over the past few years lipid nanoparticles have been especially considered, because these are composed of natural or synthetic lipids, show good biocompatibility and have potential to exhibit controlled release of drugs (Li et al., 2009). Lipid-based nanoparticle formulations may also enhance drug absorption via improvement in dissolution and solubilization within the intestinal milieu, a reduction in gastric emptying rate and increase in mucosal permeability. Lipids are known to enhance lymph formation and simultaneously promote lymph flow rate (Suresh et al., 2007). Therefore, lipid nanoparticles have the potential to enhance the overall extent of absorption as well as increase the proportion of what is absorbed and transported to the systemic circulation via intestinal lymph (Humberstone and Charman, 1997; Aungst, 2000).

Simvastatin (SV), a lipophilic active constituent derived from fungi, is a 3-hydroxy-3-methylglutaryl coenzyme A reductase inhibitor with beneficial effects on coronary diseases and mortality rate in patients with hypercholesterolemia. It is administered as an inactive lactone prodrug and has two separate metabolic pathways. Oxidative biotransformation is one of the pathway mediated primarily by cytochrome P3A (Christains et al., 1998), and hydrolyzation of simvastatin acid by carboxylesterase is another pathway leading to non-enzymatic metabolism into an active competitive statin. The SV then reduces the amount of mevalonic acid, a precursor of cholesterol, thereby inhibiting *de novo* synthesis of cholesterol. Consequently, the synthesis of low density lipoproteins receptors increases while cholesterol synthesis decreases; resulting in the increased clearance of low density lipoproteins from the bloodstream (Lilja et al., 2004).

Most of the available statins, including simvastatin, have been developed as immediate-release formulations. However, SV is a poorly water soluble drug (aqueous solubility ≈ 0.03 g/L) with a short half-life time of about 2 h, and is cleared by extensive metabolism in the intestinal gut and liver by cytochrome P 3A (Mahley and Bersot, 2006). Due to the slow dissolution rate in the intestinal tract and significant first-pass effect, the oral bioavailability of SV in humans is as low as 5%. Recently number of

* Corresponding author at: Rajiv Academy for Pharmacy, Delhi-Mathura Bypass, P.O. Chattikara, Mathura, Uttar Pradesh 281001, India. Tel.: +91 565 2913018; fax: +91 565 2825050.
E-mail address: kamla_rap@yahoo.co.in (K. Pathak).

0378-5173/$ – see front matter © 2011 Elsevier B.V. All rights reserved.
doi:10.1016/j.ijpharm.2011.05.044

strategies have been employed to address the issues related to low bioavailability and poor aqueous solubility of SV. These include self microemulsifying drug delivery system (Kang et al., 2004; Patil et al., 2007), self nanoemulsifying granules (Dixit and Nagarsenker, 2008), solid dispersion (Silva et al., 2010), cubic nanoparticles (Lai et al., 2009), and Polyring device (Vishwanathan, 2008).

In a series of investigations carried out in our lab, SV loaded SLN formulations have been worked out as a potential oral therapeutic carrier system. SLNs were formulated and optimized using two lipids, glyceryl monostearate (GMS) and Compitrol 888 ATO. The optimized SLN formulation made with GMS exhibited a particle size of 258.5 nm, %entrapment efficiency of 75.81%, with 82.67% cumulative drug release after 55 h and its recrystallization index was found to be 65.51% (Shah and Pathak, 2010). A 1.87 folds increase in bioavailability was recorded with SV SLN made using glyceryl monostearate with respect to SV suspension in. On the other hand, the optimized formulation of Compitrol based SLN with a mean particle size of 271.18 nm, %EE of 68.16% and %CDR of 76.23% after 55 h documented a relative bioavailability of 220%, substantiating the protective action of SLNs against liver metabolism. On comparison, it was concluded that the SLNs made with Compitrol 888 ATO demonstrated higher bioavailability than SLNs made with GMS because of higher lipophilic nature of the former that was responsible for more sustained release of drug (Shah et al., 2010). Though these formulations provided sustained release of SV with potential for improved therapeutic efficacy, SLNs suffer from two major limitations that are limited drug loading and expulsion of drug during storage.

Among the lipid-based formulations, the nanostructured lipid carriers (NLCs), regarded as the second-generation of lipid nanoparticles, are attracting foremost consideration as alternative colloidal drug carriers. NLCs have evolved from solid lipid nanoparticles (SLN) and are composed of a mixture of spatially different lipid molecules, i.e., solid lipid is blended with liquid lipid to overcome the disadvantages of SLNs such as limited drug loading, larger particle size, risk of gelation and drug leakage during storage caused by lipid polymorphism. In view of this NLC may be regarded as an alternative to SLN and can be exploited as a novel approach for improving the delivery of SV. Lipid formulations loaded with poorly water-soluble drugs for oral route have been investigated and reported to improve the oral bioavailability by many research teams (Mohamed et al., 1998; Paliwal et al., 2009) but there are few reports on NLC system for oral administration. In this study we have made efforts to investigate the feasibility of improving oral bioavailability of SV through NLC.

Thus the objective of present study was to develop and optimize NLC suspension of SV using solid lipid and liquid lipid agents, in order to increase the drug entrapment efficiency and to further reduce the particle size; the major limitations of SLNs and thereby increase bioavailability by preventing hepatic first pass metabolism up to some extent along with comparison with the SLN and drug suspension. Thus, the SV-loaded NLCs were developed and screened and the physicochemical characteristics, *in vitro* drug release properties, pharmacokinetics and biodistribution were investigated in detail. Then all the parameters of NLCs were compared with the SLNs. Finally, the possible absorption mechanism of NLC formulation is discussed.

2. Materials and methods

2.1. Materials

Simvastatin was a kind gift from Ranbaxy Laboratories, India. Glycerol monostearate (M.P. 52–54 °C; molecular weight 358.63) was purchased from CDH, India. Poloxamer 407 (molecular weight 12.5) was purchased from BASF, USA. Oleic acid was purchased from Ranbaxy fine chemicals limited, India. Dialysis bag (molecular weight cut off 12–14 kDa; pore size 2.4 nm) was supplied by Hi Media, Mumbai, India. Other chemicals were of analytical grade.

2.2. Experimental design

In this study, a 2^3 full-factorial design was used to optimize NLCs. In order to optimize, the amount of GMS (X_1), amount of OA (X_2) and concentration of poloxamer 407 (X_3) were selected as independent variables. Each factor was set at a high level and low level. The actual values and coded values of different variables are given in Table 1. Eight formulations of simvastatin NLCs (F1–F8) were prepared according to the factorial design. The particle size, %entrapment efficiency and %cumulative drug release at 55 h were taken as response parameters. The statistical analysis of responses was made by Design expert 8.0.2. (Stat-Ease Inc., USA) that has been detailed in Section 2.7.

2.3. Preparation of simvastatin loaded NLCs

Nanostructured lipid carriers were prepared by solvent injection technique. Simvastatin (SV) (15 mg) and specified amount of GMS and OA as given in Table 1 were dissolved in 2 ml of isopropyl alcohol (boiling point 81–83 °C) with heating at the melting temperature of GMS. Though GMS is soluble in IPA it requires some heat for ease of solubilization. The resulting solution was rapidly injected into the 10 ml of aqueous phase containing specified amount of poloxamer 407 as given in Table 1 that was continuously stirred at 400 rpm for 30 min on a magnetic stirrer. 0.1 N HCl (4 ml) was added to the dispersion to decrease the pH around 1.5–2 for causing aggregation of NLCs for the ease of separation. Thereafter, the dispersion was centrifuged at 10,000 rpm (5590 × *g*) for 30 min at 10 °C in REMI cooling centrifuge (Model C-24BL, VACO-779, Vasai, India), and aggregates were re-suspended in 10 ml double distilled water containing 4% poloxamer 407 (by weight) as stabilizer with stirring at 1000 rpm for 10 min.

2.4. Purification of SV-loaded NLCs

Purification of SV-loaded NLCs was done by dialysis technique. Re-suspended suspension was taken in the dialysis bag and sealed at both ends. The dialysis bag then immersed into 100 ml of double distilled water containing 0.2% (w/v) sodium lauryl sulphate and stirred at 100 rpm for 20 min. Five milliliter of sample was withdrawn at time intervals of 5, 10, 15, and 20 min, diluted appropriately and analyzed for amount of drug by HPLC. Paired *t*-test was used to check any significant difference between the percent free drug removed at 15 and at 20 min.

2.5. HPLC assay for SV

The SV content was assayed using ADEPT HPLC systems – Cecil CE 4201, equipped with a Rheodyne injector Hamilton 702 NR, Adept 4100 dual piston pump and detector CE 4200 set at 239 nm, with a microsorb C18 analytical column (RP-18, 250 mm × 4.6 mm, 5 μm). The mobile phase was a mixture of acetonitrile:0.01 M ammonium acetate buffer (35:65, v/v), eluted at a flow rate of 1.0 ml/min and a sample injection volume of 20 μl. The limit of detection and the limit of quantification of this analytical method were 0.163 μg/ml and 0.493 μg/ml respectively. Linear calibration curve was obtained for SV with $r^2 = 0.9998$ in the range 5–25 μg/ml.

Table 1
2^3 Full-factorial design of simvastatin-loaded NLCs, and formulation of G-SLN and C-SLN and evaluated response parameters ($n = 3$).

Formulation code	GMS X_1	OA X_2	Poloxamer 407 X_3	Particle size (nm)	%EE	Zeta potential[a] (mV)	PDI[a]	%CDR after 55 h
F1	−1	−1	−1	209.9	83.91 ± 2.25	−31.1	0.355	73.65 ± 2.54
F2	−1	−1	+1	206.7	82.92 ± 1.13	−32.1	0.351	81.23 ± 2.76
F3	−1	+1	−1	194.4	93.33 ± 3.26	−35.8	0.242	88.34 ± 3.23
F4	−1	+1	+1	180.9	86.49 ± 2.83	−39.8	0.250	91.49 ± 3.78
F5	+1	−1	−1	260.0	88.64 ± 1.61	−29.1	0.191	57.95 ± 3.18
F6	+1	−1	+1	254.9	81.74 ± 3.45	−35.4	0.359	59.13 ± 4.11
F7	+1	+1	−1	239.4	91.46 ± 1.02	−39.1	0.360	65.59 ± 3.12
F8	+1	+1	+1	230.6	90.54 ± 2.91	−30.2	0.371	69.98 ± 3.76
F9	0	0	0	211.54	83.97 ± 3.46	−34.5	0.344	77.81 ± 4.20
G-SLN	−1	–	0.38	258.5	75.81 ± 4.54	−22.34	0.245	82.67 ± 3.46
C-SLN	−1	–	0.57	271.18	68.16 ± 3.88	−25.94	0.361	76.23 ± 3.33

Actual values: X_1, +1 = 200 mg, −1 = 100 mg, 0 = 150 mg; X_2, +1 = 30 mg, −1 = 15 mg, 0 = 22.5 mg; X_3 (%, w/w), +1 = 0.8%, −1 = 1.2%, 0 = 1.0%, 0.38 = 1.1%, 0.57 = 1.1%.
[a] Not selected for the optimization.

2.6. Characterization of NLC

2.6.1. Particle size and zeta potential

The particle size and zeta potential of the formulations were determined by laser scattering technique using Malvern Hydro 2000SM (Malvern Instruments, UK) after appropriate dilution with double distilled water. Light scattering was measured at an angle of 90°. The aqueous nanoparticulate dispersion was added to the sample dispersion unit containing stirrer and stirred to minimize the interparticle interactions, while the laser obscuration range was maintained between 10% and 20%.

2.6.2. Entrapment efficiency

In order to determine the entrapment efficiency, the equation reported by Shah and Pathak (2010) was utilized, and %EE was calculated by the following equation:

$$\%EE = \left[W_a - \frac{(W_s + W_p)}{W_a} \right] \times 100 \quad (1)$$

where W_a is the amount of drug added in system, W_s is the amount of drug in supernatant after the centrifugation, and W_p is the amount of drug in the purification medium.

2.6.3. In vitro drug release

In vitro drug release study of NLCs was performed by dialysis bag diffusion technique. NLC-suspension equivalent to 5 mg SV was filled in dialysis bag and immersed in a receptor compartment containing 100 ml of phosphate buffer, pH 7.4, stirred at 100 rpm and maintained at a temperature of 37 ± 0.5 °C. The receptor compartment was covered to prevent evaporation of the medium. Five milliliter of aliquots were withdrawn at various time intervals (1, 2, 3, 4, 5, 6, 7, 8, 9, 10, 11, 23, 24, 25, 26, 27, 28, 29, 30, 31, 32, 33, 34, 35, 48, 49, 50, 51, 52, 53, 54 and 55 h), and replaced with fresh volume of dissolution medium, diluted appropriately, and concentration was measured by HPLC at 239 nm. The experiments were performed in triplicate.

2.7. Statistical analysis of responses by design expert

Design Expert 8.0.2. (Stat-Ease Inc., USA) was used for the analysis of effect of each variable on the designated response. Pareto charts were made for the analysis of each response coefficient for its statistical significance. Quantitative and qualitative contribution of each variable on each of the response was analyzed. The significant polynomial equations generated by Design Expert were used to validate the statistical design (Bolton and Bon, 2004). Validation of design of SV-NLC was done by preparing extra design check point formulation (F9), and for that center point of each variable level was selected. This coded level was transformed to actual value of each variable using principle of transformation. Experimental value and predicted value of each response were determined by performing experiment and using design expert software respectively. Response surface plots were generated to visualize simultaneous effect of each variable on each response parameter.

2.8. Selection of optimized formulation

For the selection of optimized formulation, Design Expert software was utilized. It is an advantageous tool, which varies each variable simultaneously and gives all possible optimum selections based on which the optimized formulation is selected. Thus, optimized formulation was selected on the basis of small particle size, higher entrapment efficiency, and higher *in vitro* cumulative drug release after 55 h.

2.9. Characterization of the optimized formulation

Besides particle size, zeta potential, entrapment efficiency and *in vitro* release, additional investigations including electron microscopy, differential thermal analysis, radiolabeling and pharmacokinetic and tissue uptake studies were performed on selected optimized formulation (F4).

2.9.1. Transmission electron microscopy

The morphology of SV-NLC suspension was observed by transmission electron microscopy [Hitachi (H-7500) 80 kV, Japan]. The sample was prepared by placing a drop of SV-NLC that was previously diluted 50-folds with double-distilled water onto a 400-mesh copper grid coated with carbon film and followed by negative staining with 1% phosphotungstic acid. The sample was dried in the air before TEM observation.

2.9.2. Differential thermal analysis

In order to evaluate the recrystallization index, differential scanning calorimetry was performed using Universal V4.5A TA differential scanning calorimeter. Accurately weighed sample(s) was placed in aluminum pan and sealed with a lid. Aluminum oxide was used as the reference. In the scanning process, a heating rate of 10 °C/min was applied in the temperature range from −50 °C to 200 °C with a nitrogen purge of 0.2 ml/min. The recrystallization index (RI) was computed by the following equation (Souto et al., 2006):

$$\%RI = \frac{\Delta H_{NLC}}{\Delta H_{bulk\ lipid} \times \text{ fraction of lipid phase}} \times 100 \quad (2)$$

where ΔH_{NLC} is enthalpy of fusion of NLC, and $\Delta H_{bulk\ lipid}$ is enthalpy of fusion of GMS.

2.9.3. Radiolabeling of formulations

Radiolabeling of simvastatin suspension and optimized simvastatin NLCs was done by direct method using stannous chloride as reducing agent. Briefly, 1 ml of simvastatin suspension and optimized simvastatin NLCs was mixed with stannous chloride. To adjust the pH of this mixture, 10 μl of sodium hydrogen carbonate solution was added. Then, 0.1 ml of freshly eluted Tc-99m (Regional Center for Radiopharmaceuticals, BRIT, New Delhi, India) (1.5 mCi) was added to each preparation, mixed well, and incubated at room temperature. Final radioactivity present in the preparation was checked using gamma ray counter (Capintech, CAPRAC-R, USA).

2.9.3.1. Optimization of radiolabeling efficiency. The effect of the amount of stannous chloride, the final pH of the preparation, and the incubation time on labeling efficiency was optimized by changing one parameter at a time. For optimizing amount of stannous chloride, a range of 25–400 μg of stannous chloride was used. Similarly, pH of the reaction mixture was varied from 4 to 7 and incubation time was varied between 5 and 30 min.

2.9.3.2. Determination of labeling efficiency. The labeling efficiency of simvastatin suspension, and optimized simvastatin NLCs was determined by ascending thin layer chromatography (TLC) using instant thin-layer chromatography (ITLC) strips coated with silica gel (Gelman Science Inc., Ann Arbor, MI). The ITLC strips were spotted with 1–2 μl of labeled complex at 1 cm above the bottom. These strips were developed using solvent system (pyridine:acetic acid:water ion ratio of 3:5:1.5) to determine free Tc-99m. The solvent front was allowed to reach to a height of approximately 6–8 cm from the origin, and, the strip was cut horizontally into two halves. Radioactivity in each half was determined by using gamma ray counter.

2.9.3.3. Stability study of labeled complex. Stability of the Tc-99m labeled simvastatin suspension and optimized simvastatin NLCs was determined *in vitro* in mice serum and normal saline by ascending TLC technique. The labeled complex (0.1 ml) was incubated separately, with 0.9 ml freshly collected mice serum and 0.9 ml normal saline separately at room temperature. Aliquots samples were withdrawn at time intervals of 1, 2, 4, 24 and 48 h and ITLC was performed. These strips were counted for radioactivity. The preparations were stable in mice serum and normal saline for 48 h. At all time points 99Tcm labeled preparations demonstrated radiolabeling efficiency of more than 96%.

2.9.4. Pharmacokinetics and tissue uptake study

All animal experiments were carried out according to the principles of Committee for the Purpose of Control and Supervision of Experiments on Animals (CPCSEA) Chennai, India. The protocols for the animal studies were approved by the Institutional Animal Ethical Committee (IAEC) Ref No-IAEC/RAP/2908/2010 of Rajiv Academy for Pharmacy Mathura, India. Balb/C mice weighing 25–30 g were obtained from Animal Experimental Center of Institute of Nuclear Medicines and Allied Sciences, New Delhi and housed at a temperature of 22 ± 2 °C and 45–50% relative humidity.

The mice were divided randomly into two groups (group 1 and group 2) comprising fifteen animals each and fasted overnight, but allowed to free access to water before experiment. The radiolabeled SV-suspension and optimized SV-NLCs with a final radioactivity of 1.5 mCi/ml (equivalent to the dose of 5 mg/kg of simvastatin) was administered orally to group 1 and group 2 animals respectively. For pharmacokinetic evaluation, the mice were anaesthetized using chloroform at 1, 2, 4, 24, 48 h post administration and blood was collected via cardiac puncture. For tissue uptake study at each time point, three mice were sacrificed and organs of interest such as liver, lungs, spleen, kidney, heart, intestine and stomach were quickly removed. The organ samples including blood were analyzed for radioactivity by gamma ray counter. Radioactivity in the sample was determined in the unit of counts/minute and % uptake per gram organ weight was calculated by the following equation:

$$\%\ \text{uptake/gram organ weight} = \frac{[\text{counts/weight}] \times 100}{\text{total administered counts}} \quad (3)$$

The pharmacokinetic parameters were acquired with the help of pharmacokinetic program Quickcal software (Plexus, Ahmadabad, India). The relative bioavailability of NLC formulations was calculated using the following equation:

$$\text{Fr}\ (\%) = \frac{\text{AUC}_{\text{SV-NLC}}}{\text{AUC}_{\text{SV-suspension}}} \times 100 \quad (4)$$

where Fr (%) is the relative bioavailability, AUC is the area under the plasma concentration–time curve. Various pharmacokinetic parameters such as C_{max}, T_{max}, elimination half life, absorption constant, elimination constant volume of distribution and clearance were also calculated.

2.9.5. In vitro in vivo correlation

The percentage of SV absorbed at specific times was calculated from the blood concentration data using the Wagner and Nelson method. The method was based on utilization of the following equation:

$$\frac{A_T}{V_d} = C_T + K_{el}(\text{AUC})_{t=0-T} \quad (5)$$

where A_T is the amount of drug absorbed at time t, V_d is the apparent volume of distribution, C_T is the blood concentration at time $t = T$, K_{el} is the elimination rate constant and AUC is the area under the curve between the limits $t = 0$ to $t = T$. A value of $K_{el} = 0.134\ h^{-1}$ was calculated from the slope obtained by a least-squares regression of the linear region of the log blood %A/G versus time profile for free SV suspension after oral dosing. Using this method, successive values of A_T/V_d were calculated to obtain the maximum $(A_T/V_d)_\infty$, which was then divided into each value of A_T/V_d to determine the percentage absorption data as a function of time.

3. Results

3.1. Formulation considerations

NLCs were prepared by solvent injection technique that relies on rapid diffusion of the solvent across the solvent–lipid interfaced with the aqueous phase and this physical phenomenon is critical for the nanosized lipid particle precipitation. Owing to their small size coupled with low density of lipids, NLCs present difficulty in settling upon centrifugation. To overcome this limitation, in the present study, the pH of the dispersion was reduced to 1.5–2 to adjust the zeta potential to a level that promotes aggregation of nanosized particles, facilitates centrifugation and consequently separation. Another significant aspect in preparation of NLCs is purity of the product obtained. A possibility of presence of free simvastatin particles in the sediment of simvastatin-loaded NLCs cannot be denied and hence was explored. Free drug particles can affect both, the *in vitro* and *in vivo* release behavior of simvastatin. Therefore, free drug particles were removed from the sediment of NLCs by dialysis technique. This technique was considered suitable, as simvastatin with a low molecular weight of 418.57 Da could be efficiently removed using dialysis bag made of the membrane with cut off 12–14 kDa. Consequently, purification was accomplished by monitoring percent free drug removed with respect to time. Initially, the percent free drug removed increased linearly with time and reached plateau levels within 20 min. Paired *t*-test was used to check any significant difference between the percent free

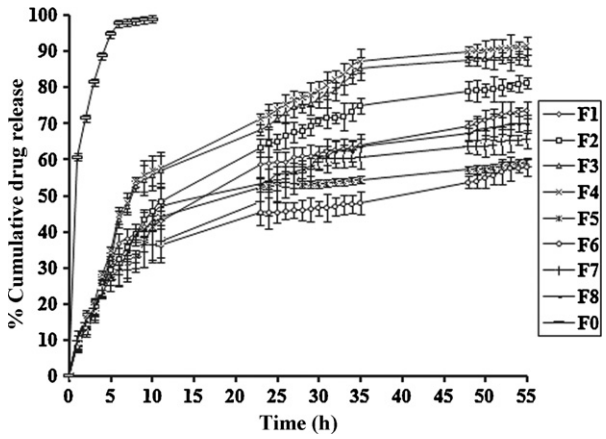

Fig. 1. *In vitro* release profiles of suspension (F0) and NLCs of simvastain (F1–F8) in phosphate buffer, pH 7.4.

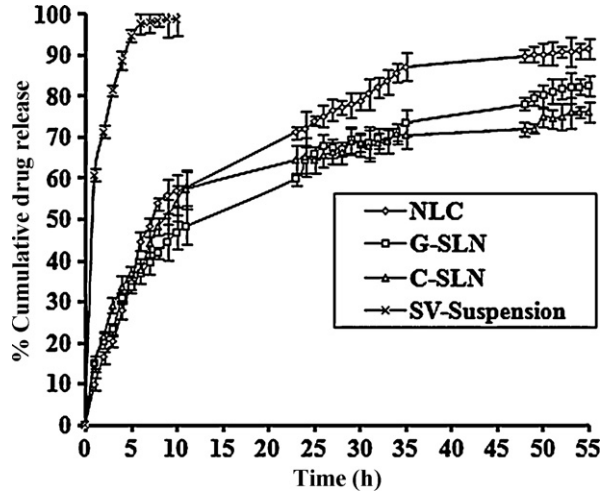

Fig. 2. Comparative *in vitro* release profiles of NLCs, G-SLN, C-SLN and SV-suspension in phosphate buffer, pH 7.4.

drug removed at 15 and 20 min and no significant difference was observed ($p > 0.01$). Thus, free SV from sediment of NLCs could be efficiently removed by dialysis for 15 min and was used throughout the experiment.

3.2. Analysis of dependent variables

3.2.1. Particle size and zeta potential

Values of the particle size and surface charge of the developed NLCs are documented in Table 1. The results showed that the amounts of GMS and OA were critical parameters in governing the particle size. After production, the mean diameter of the particles ranged between 180.9 and 260 nm and polydispersity was between 0.191 and 0.371. The mean particle size was least when GMS was at low level and OA and poloxamer were at high levels (F4) and the particle size was largest when GMS was at high level and both OA and poloxamer were at low levels (F5). Thus, upon increasing the OA percentage in the lipid matrix from 15% to 30%, the mean particle size decreased. Hence F4 was the smallest sized nanostructured lipid nanoparticle with a zeta potential of −39.8 mV. As depicted in Table 1, the zeta potential values closely ranged between −29.1 and −39.8 mV. Least value of zeta potential was associated with F5 and the highest with F4 and rest of the formulations showed intermediate values.

3.2.2. Drug entrapment efficiency

An important issue with respect to the use of nanoparticles as drug carriers is their capacity for drug loading and consequently the effects of OA concentration on drug entrapment efficiency were investigated. It is clear that the entrapment efficiency of nanoparticles increased from 81.74% to 93.33% respectively upon increasing the percentage of OA from 15 to 30 wt%. These values are considerably higher than the encapsulation efficiency of SLN made with SV in our lab. The entrapment efficiency of optimized SLNs made with glyceryl monostearate (Shah and Pathak, 2010) and Compitrol 888 ATO (Shah et al., 2010) was 75.81% and 68.16% respectively (Table 1). Thus, incorporation of OA in lipid matrix resulted in higher entrapment efficiency as compared to SLN.

3.2.3. In vitro drug release

In order to develop a prolonged release system, it is vital to understand the release mechanism and kinetics. The *in vitro* SV release profiles of F1–F8 and SV suspension (F0) are shown in Fig. 1. The *in vitro* release profiles of the test formulations (F1–F8) were different from the reference formulation F0 (*f2* ranged between 92 and 96). The cumulative amount of SV released from each formulation was plotted as a function of time and as evident the SV suspension showed quick release of simvastatin, with a cumulative release of more than 90% within 6 h. On the other hand the release of SV from the NLCs (F1–F8) slowed down considerably and it varied from 57.95% to 91.49% in 55 h depending upon the GMS/OA levels. As is evident, formulation F4 formulated using low levels of GMS and high levels of both OA and poloxamer 407 displayed highest %CDR (88.3% ± 3.23) that was quite in contrast to formulation F5 formulated with high levels of GMS and low levels of both OA and poloxamer 407 exhibited least %CDR (57.95% ± 3.18) after 55 h. The release profiles were not smooth curves but were identified as biphasic with initial faster release phase till 10 h followed by a slower release phase thereafter till 55 h. On comparing the release

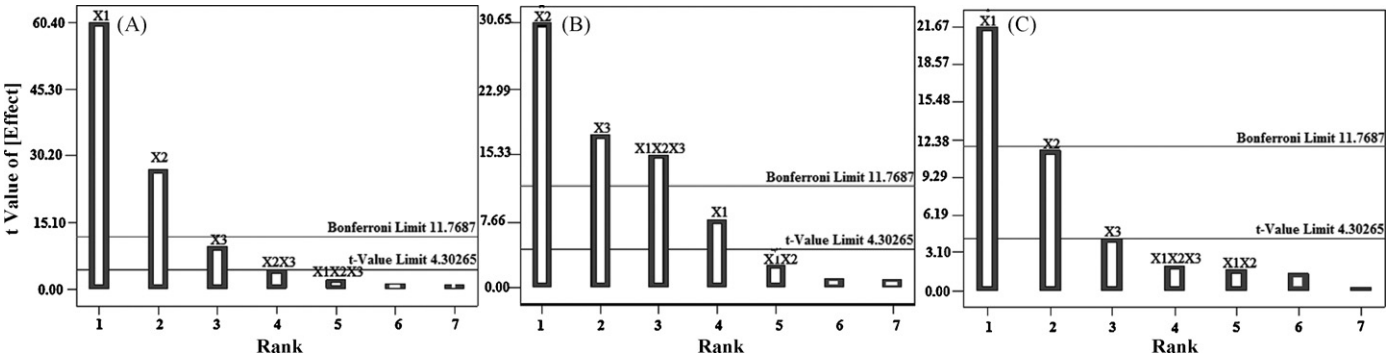

Fig. 3. Pareto charts for analysis of response coefficient significance on the dependent variables (a) particle size, (b) %EE, and (c) %CDR.

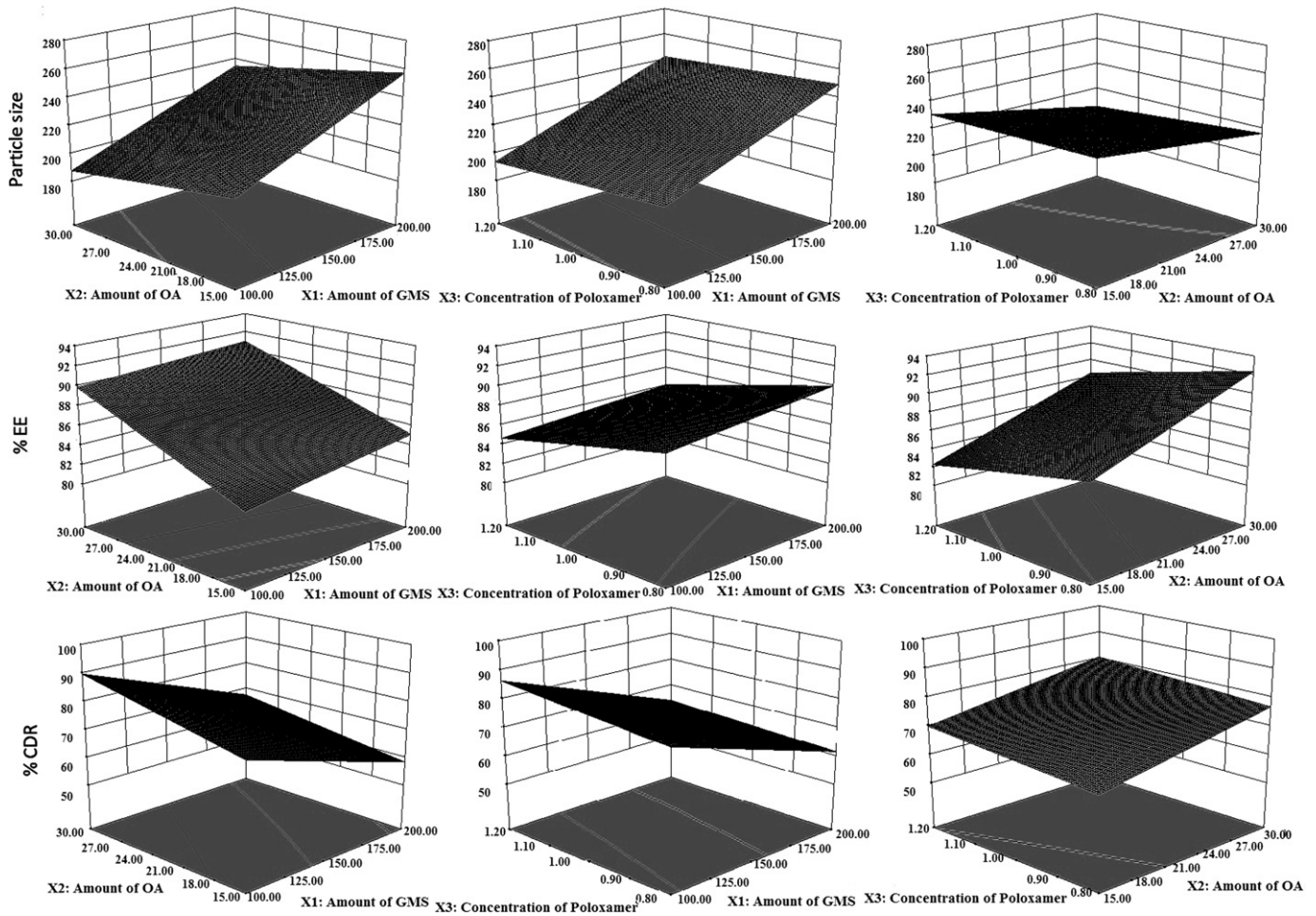

Fig. 4. Response surface plots showing simultaneous influence of independent variables on response parameters of SV loaded NLC formulated within the experimental design.

trends of optimized SLNs (G-SLN (glyceryl monostearate SLN) and C-SLN (Compritol 888 ATO SLN) with NLC (Fig. 2), evidently the release patterns were similar but the quantum of release was higher in case of SV NLC than SV SLNs. The SLNs exhibited <80% release in 55 h whereas NLC release >90% of SV in 55 h. Consequently, F4 that displayed maximum %CDR within 55 h and based on the evaluation of the three dependent variables, the optimized formulation F4 was selected as the optimized formulation.

3.3. Validation of experimental design

The selected independent variables like the amount of GMS, amount of OA and concentration of poloxamer 407 influenced the particle size, %EE, and %CDR that is quite evident from the results in Table 1 and has been documented in preceding sections. Consequently, for each dependent variable, the response polynomial coefficients were determined in order to evaluate the effect of each response. Each response coefficient was studied for its statistical significance by Pareto charts as shown in Fig. 3. Pareto charts establish t value of effect that is studied by two limit lines namely the Bonferroni limit line (t value of effect = 3.082) and t limit line (t value of effect = 2.1199). Coefficients with t value of effect above the Bonferroni line are designated as certainly significant coefficient; coefficients with t value of effect between Bonferroni line and t limit line are termed as coefficients likely to be significant, while t value of effect below the t limit line is statistically insignificant coefficient and are removed from the analysis. Thus, non-significant response coefficients were deleted and following significant polynomial response equation(s) for particle size, %EE, and %CDR were generated.

$$\text{Particle size (nm)} = 222.10 + 24.11X_1 - 0.78X_2 - 3.84X_3 - 1.76X_2X_3 + 0.83X_1X_2X_3 \quad (6)$$

$$\%\text{EE} = 87.27 + 0.83X_1 + 3.19X_2 - 1.84X_3 + 1.59X_1X_2X_3 \quad (7)$$

$$\%\text{CDR} = 73.41 - 10.26X_1 + 5.43X_2 + 2.04X_3 - 0.80X_1X_2 + 0.95X_1X_2X_3 \quad (8)$$

These equations were utilized for validation of the experimental design by formulating an extra design checkpoint formulation F9. Utilizing the above equations, particle size of 222.10 nm, entrapment efficiency of 87.27% and %CDR of 73.41% at 55 h were predicted. Experimental run of F9 yielded values close to the predicted indicating validity of the generated model. To further analyze the effect of variables on the responses, response surface plots (Fig. 4) were generated that represent the simultaneous effect of any two variables on response parameter taking one variable at constant level. On carefully observing these plots, the qualitative and interactive effect(s) of independent variables on each response parameter can be visualized and the results are summarized in Table 2.

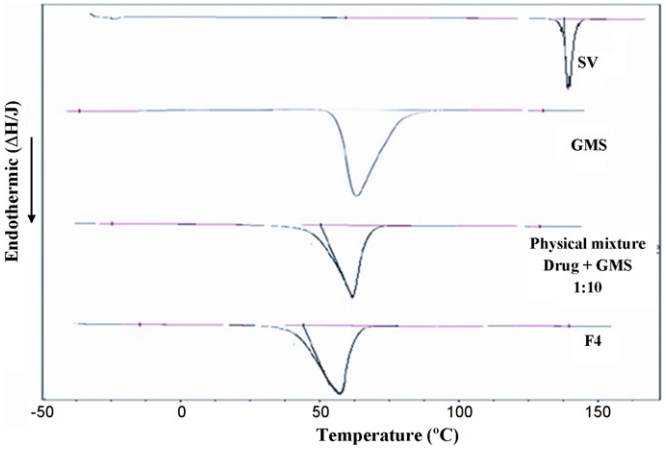

Fig. 5. Differential scanning calorimetric profiles of SV, GMS, SV-GMS physical mixture and the formulation F4.

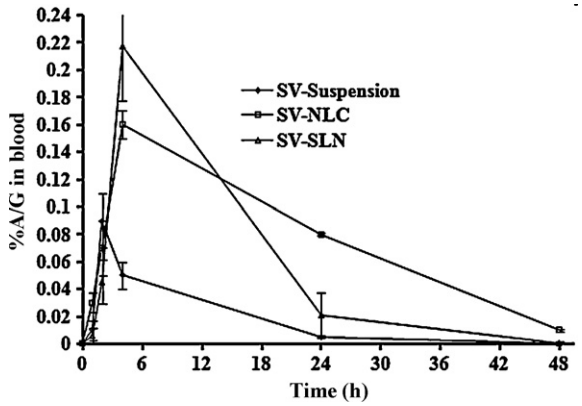

Fig. 6. %A/G in blood versus time profile of SV suspension, SLN and NLC after oral administration of the radiolabeled formulations in mice.

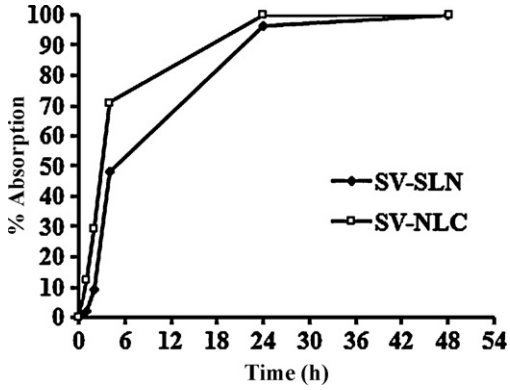

Fig. 7. Absorption profiles of SV loaded NLC and SLN generated from deconvolution of the corresponding blood concentration profiles using the Wagner–Nelson method.

3.4. Recrystallization index

Examination by DSC patterns (Fig. 5) revealed single peaks in the endotherms of SV (m.pt = 139.6 °C; ΔH = 71.19 J/g) and glyceryl monostearate (m.pt = 57.65 °C; ΔH = 79.19 J/g). The endotherm of F4 recorded a distinctive broad, slightly asymmetric single peak at 54.95 °C with ΔH of 29.1 J/g and the peak for SV was not evident. The melting point of the developed formulation was lower than that of bulk GMS; however, there was a detectable melting event over 50 °C confirming solid state of the lipid matrix at room temperature. The shift in melting point of NLC may attributed either to the interaction of solid lipid with the liquid lipid and the surfactants, or due to the colloidal size range of the lipid particles. The disappearance of melting peak in the endotherm of F4 can be explained by Kelvin effect, according to which small, isolated particles (SV) would melt at a temperature lower than the melting temperature of bulk material (glyceryl monostearate). As the differential scanning analysis was aimed at evaluating changes upon storage, the enthalpy values were utilized for calculating recrystallization index (RI). The RI of F4 was calculated as 36.71% against the reference value of 100% for GMS that was much lower than the RI of 91.1% for physical mixture of SV and GMS (1:10). It is clear that the recrystallization of optimized NLC formulation was depressed by the addition of the OA that decreased crystallinity, promoted disordered arrangement and consequently reduced the tendency of solid lipid to recrystallize.

3.5. Pharmacokinetic study

The blood %A/G–time plots, in mice after oral administration of test formulations (SV suspension, SV-SLN and SV-NLC) are shown in Fig. 6 and the pharmacokinetic parameters are tabulated in Table 3. The T_{max} was 2 h and the C_{max} was 0.09%A/G after oral administration of SV suspension. However, the time to achieve maximum concentration of SV was delayed by 2 h in both case of NLC and SLN. The C_{max} of SV-NLC was 0.16%A/G which was significantly ($p > 0.01$) higher than that obtained with the SV suspension (0.09%A/G) but lower than SLN (1.24%A/G). Meanwhile, at all time points, the %A/G in blood of SV-NLC were remarkably higher than those administered with SV suspension. Twenty-four hours after oral administration of SV-NLCs, the blood %A/G was still 0.08%, whereas the activity was undetectable 24 h after administration of SV suspension and was much lower in case of SLN. The $AUC_{(0-\infty)}$ of SV-NLC was 3.92%A/G/h, that was 4.87 folds higher than $AUC_{(0-\infty)}$ of 0.804%A/G/h for SV suspension and 2.74 times more than SLN formulation of SV, clearly defining performance superiority of NLC over SLN and suspensions. Lower values of V_d for NLC in comparison to SLN and suspension are indicative of larger fraction of formulation being retained in the central compartment and hence more bioavailable.

Table 2
A compilation of interactive status and simultaneous qualitative effect of independent variables on each response parameter.

Parameter	Assessment of	Interacting variables		
		X_1X_2	X_1X_3	X_2X_3
Particle size	Interaction	–	–	+
	Effect on dependent variable	Increase	Increase	Decrease
Percent entrapment	Interaction	+	–	–
efficiency	Effect on dependent variable	Increase	Increase	Increase
Percent CDR in 55 h	Interaction	+	+	–
	Effect on dependent variable	Decrease	Decrease	Increase

(–) antagonistic interaction, (+) synergistic interaction.

Table 3
Pharmacokinetic parameters of radiolabeled SV-suspension, NLC and SLN after oral administration of the test formulations.

Evaluation parameters	SV-suspension	NLC	SLN
C_{max} (%A/G)	0.09 ± 0.02*	0.16 ± 0.04	1.24 ± 0.076*
T_{max} (h)	2*	4	4
Elimination half life (h)	5.20 ± 1.2*	10.86 ± 1.74	6.72 ± 2.69*
Absorption constant (h^{-1})	0.32 ± 0.094	0.31 ± 0.082	0.13 ± 0.011*
Elimination constant (h^{-1})	0.134 ± 0.09*	0.06 ± 0.092	0.12 ± 0.08*
Volume of distribution (L)	9.3 ± 2.3*	4.0 ± 1.3	6.89 ± 2.21*
Clearance (L/h)	1.24 ± 1.3*	0.26 ± 0.9	0.713 ± 0.97
$AUC_{(0-\infty)}$ (%A/G/h)	0.804 ± 0.65*	3.92 ± 1.1	1.43 ± 1.43*
Relative bioavailability (%)	100*	488	186*

Each value represents the mean ± SD ($n = 3$); *$p < 0.01$, comparison with NLC.
The table shows the mean and SD ($N = 3$) of pharmacokinetic parameters calculated following oral administration of SV suspension, NLC and SLN in Balb/C mice. The p values for each parameters is an unpaired t-test comparison among SV suspension, NLC, and SLN after oral delivery [<0.01 (*)].

3.6. *In vitro–in vivo correlation*

Correlation between *in vitro* and *in vivo* data for SV-NLC and SLN was investigated. Three levels of IVIVC are classified according to the US Food and Drug Administration (Dressman and Reppas, 2000). The best correlation Level A, is point-to-point relationship between *in vitro* dissolution and *in vivo* absorption. Using Wagnor–Nelson method, the percentage absorption data as a function of time to get the plots shown in Fig. 7. The absorption profiles of both the SV NLC formulation and SLN were similar but varied in extent of absorption. The NLCs exhibited higher percent absorption of SV than SLN in the initial phase that gradually increased with time (4 h) and the difference was maintained till 24 h. Thereafter both the profiles merged into a single point in 48 h. On plotting the fraction SV absorbed against the fraction SV released from the lipid nanoparticulate system, linear correlation with R^2 values of 0.940 and 0.941 were obtained for SV-NLC and SV-SLN respectively (Fig. 8) indicating that the *in vitro* release test can be used to predict the *in vivo* performance of the developed formulations.

3.7. *Tissue uptake study*

The tissue uptake study of ^{99m}Tc labeled formulations (maximum labeling efficiency of 99.36% observed with 200 mcg/ml $SnCl_2$, pH 6–6.5 and an incubation time of 25 min) was investigated in the vital organs heart, lungs, liver, spleen, kidney, stomach and intestine and it was observed that the distribution pattern varied depending on the dosage form (Table 4). On comparing the distribution of drug from SV suspension and SV loaded NLC, higher radioactivity was demonstrable in stomach within 1 h of oral administration from both the formulations that started to decline in the second hour and diminished by the end of 24 h. Fast decline of radioactivity in stomach is attributable to short gastric residence time of SV suspension and the SV loaded NLC administered as suspension. Decline of radioactivity in stomach corresponded to increase in radioactivity in intestine due to gastrointestinal transit of suspension. In case of intestine, the radioactivity was maximum in second hour for SV suspension but for SV NLC maximum activity was seen up to 4 h after administration indicative of higher residence time of NLC in intestine that can provide an opportunity for prolonged absorption of SV from NLCs. This result is consistent with the sharp increase in the percent drug absorbed within 4 h as shown in Fig. 7.

As the drug got absorbed and distributed to various organs, the uptake pattern of radiolabeled formulations in vital organs was analyzed. The accumulation of SV NLC was higher in liver than SV suspension at all time points than from suspension. In case of SV suspension maximum activity was observed within 2 h of administration that was maintained till 24 h and declined thereafter. This is quite different from the distribution kinetics of SV-NLCs. The %A/G that was initially higher than SV suspension kept on increasing up to 24 h suggesting accumulation of NLCs in liver. This is advantageous because the liver is the target organ, to reduce the cholesterol level in blood.

In rest of the organs analyzed for biodistribution, the %A/G was not very significantly different except for few test points marked in the table. However, the radioactivity from SV NLC was grossly higher as compared to suspension in lungs, heart, spleen and kidney.

4. Discussion

NLCs of SV were formulated using a combination of highly ordered and less ordered lipids. As documented in literature, the less ordered lipid enhances the entrapment efficiency of the nanoparticulate system because entropy of the lipid provides space for entrapment of drug molecules. In present investigation OA was used as the less ordered lipid and its concentration markedly affected drug loading and also the size of NLC. Thus, at higher levels of OA (30 wt%) small, spherical nanoparticles with high entrapment efficiency were obtained. OA is considered as the main factor responsible for the reduction in particle size and decreased polydispersity index because its inclusion in the formulation led to reduction in viscosity and surface tension inside NLCs that helped in the formation of nanosized homogenously distributed nanoparticles. The nanoparticles are thermodynamically unstable systems and for the stability of colloidal drug carriers, a zeta potential value of equal to or more than 30 mV is desirable. In the present study the zeta potential of NLCs within the design closely ranged between −29.1 and −39.8 mV suggesting thermodynamically stable systems. But high zeta potential value coupled with nanosized particles presents difficulty in separation by centrifugation, so 0.1 M hydrochloric acid was added to the system to reduce zeta potential and facilitate centrifugation.

As OA affects particle size so does it affects the entrapment efficiency. Researchers have explained that the liquid lipids cause numerous crystal defects in solid lipid and provide imperfections in highly ordered crystal. In this space more drug molecules get entrapped. As both particle size and entrapment efficiency are determinants of drug release from a given carrier system, the *in vitro* drug release profiles were expected to vary accordingly. Thus, the formulation F4 with smallest particle size of 180 nm (Fig. 9) and highest entrapment efficiency displayed maximum %CDR in a sustained manner. It can be realized that OA played key role in influencing the %CDR versus time profile. Thus, at high level of OA the particle size reduced leading to increased specific surface area and consequently %CDR. The %CDR profile typically consisted of two parts, the initial faster phase followed by gradual slow release. This behavior is similar to the one documented by Zhuang et al. (2010). According to the authors, when solvent

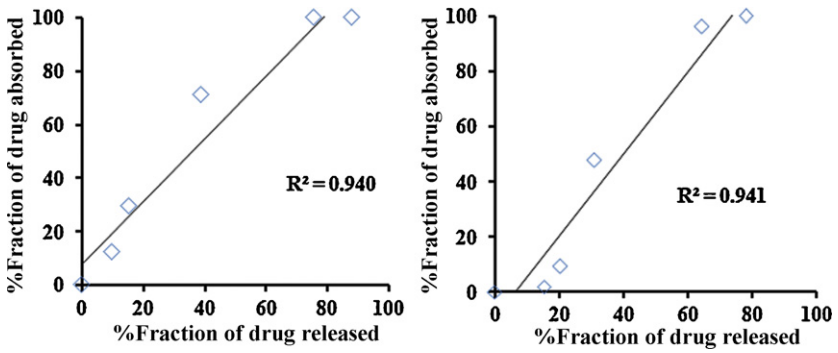

Fig. 8. *In vitro in vivo* correlation of (a) SV loaded NLC and (b) SV loaded SLN.

injection method is utilized for preparing NLCs, the difference in melting points of solid and liquid lipid, leads to the crystallization of solid lipid, forming a liquid lipid free core or a core with little lipid. Most of the liquid lipid is located at the periphery of NLCs particle. In our case this phenomenon led to formation of OA-enriched peripheral layer(s) that possesses substantially higher solubility for the lipophilic drug. Thus, simvastatin was readily loaded in higher amounts in the peripheral region and was easily released by the drug diffusion contributing to initial faster drug release phase followed by slow release from the relatively solid core. Thus, it is possible to modify the release profiles as a function of the lipid matrix and this is demonstrated in Fig. 6 where the *in vitro* release profiles of SV-SLNs made up of complete solid core of glyceryl monostearate and Compitrol 888 ATO showed slower release rate. It can be realized that the mobility of drug is drastically reduced in solidified or crystallized nanoparticles, resulting in slow drug release. Among the NLC formulations evaluated for *in vitro* release, F4 displayed maximum %CDR within 55 h and based on the evaluation of the three dependent variables, the optimized formulation F4 was selected for further investigation.

In addition to affecting the particle size, entrapment efficiency and *in vitro* drug release characteristics, the liquid lipids integrated into the solid lipids in NLCs cause reduction of ordered matrix structure and allow adequate spaces to lodge the drug molecule that is firmly embraced in the disordered structure during long-term storage (Muller et al., 2000). Thus, NLCs can offer solutions to the changes that may occur upon aging, crystallinity and polymorphism of SLNs. The recrystallization index was used as a parameter to evaluate the ability of nanostructured lipid carrier in retarding any potential changes that can occur upon long term storage. Significantly ($p < 0.001$) low value of the recrystallization index than the SLNs signified the role of liquid lipid in retarding recrystallization. As a well documented fact crystallization occurs due to supersaturation and the presence of liquid lipid probably tends to maintain subsaturation state of the solid lipid retarding crystallization. Hence, the SLNs made with GMS (Shah and Pathak, 2010) and Compitrol 888 ATO (Shah et al., 2010) had higher recrystallization tendency than NLCs of simvastatin.

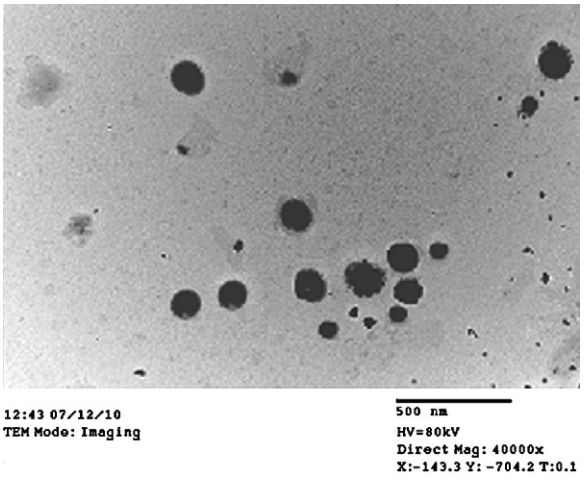

Fig. 9. Transmission electron microscopic image of the optimized SV loaded NLC (F4).

NLCs of SV had superior pharmacotechnical properties than SLNs and hence were assessed for their pharmacokinetics and biodistribution in mice using SV suspension as reference formulation. Compared to SV-suspension, the %A/G versus time profile of SV-NLC displayed a smoother %A/G versus time profile, with a delayed T_{max}, and prolonged $t_{1/2}$. This offers a chance for reduction in dosing frequency. The visible difference between T_{max} value of SV-NLC and SV suspension manifested that the rates of absorption for the formulations were not same. SV from suspension dissolved in the intestinal tract fluids and was then absorbed into the systemic circulation in contrast to SV-NLC that released SV very gradually into the gastrointestinal tract, as indicated by the *in vitro* release studies consequently leading to slow absorption. The sustained release of drug from the NLC's not only slowed down the absorption it also affected the elimination half-life of SV. Consequently the $t_{1/2}$ of SV from NLCs almost doubled than the $t_{1/2}$ of SV from suspension and even higher than the $t_{1/2}$ of SV from SLN.

Poor water-solubility, extensive hepatic first pass metabolism and the separation from the bulk aqueous phase of intestinal contents by unstirred water layer of the brush bordered membrane of the enterocytes lining the small intestine, are major barriers to absorption of poorly water soluble lipid digestion products. These are also the possible reasons of low bioavailability of simvastatin. Considering the structure of SV, a weakly alkaline compound ($pK_a = 4.7$), that shows higher solubility at low pH values, the solubility of SV throughout the gastrointestinal tract can be analyzed. After oral administration, the drug would first dissolve in the gastric fluid and present itself for absorption. When the drug reaches the intestinal tract, increase in pH will result in precipitation of the drug, that will affect the absorption. Additionally, SV that gets directly absorbed from the intestine into the blood circulation would meet extensive metabolism in the liver resulting in poor bioavailability. In the case of SV-NLC and SLN, the presystemic hepatic effect can be largely avoided because that the drug is encapsulated in nanoparticles and owing to their colloidal nature these were available for the lymphatic absorbing pathway. This can enhance the bioavailability of the drug and the sustained release property of SV-NLC and SLN could also achieve a longer retention time of drug *in vivo*.

Analysis of the composition of NLCs can also explain enhancement in the bioavailability. GMS and OA, which is similar to fat rich

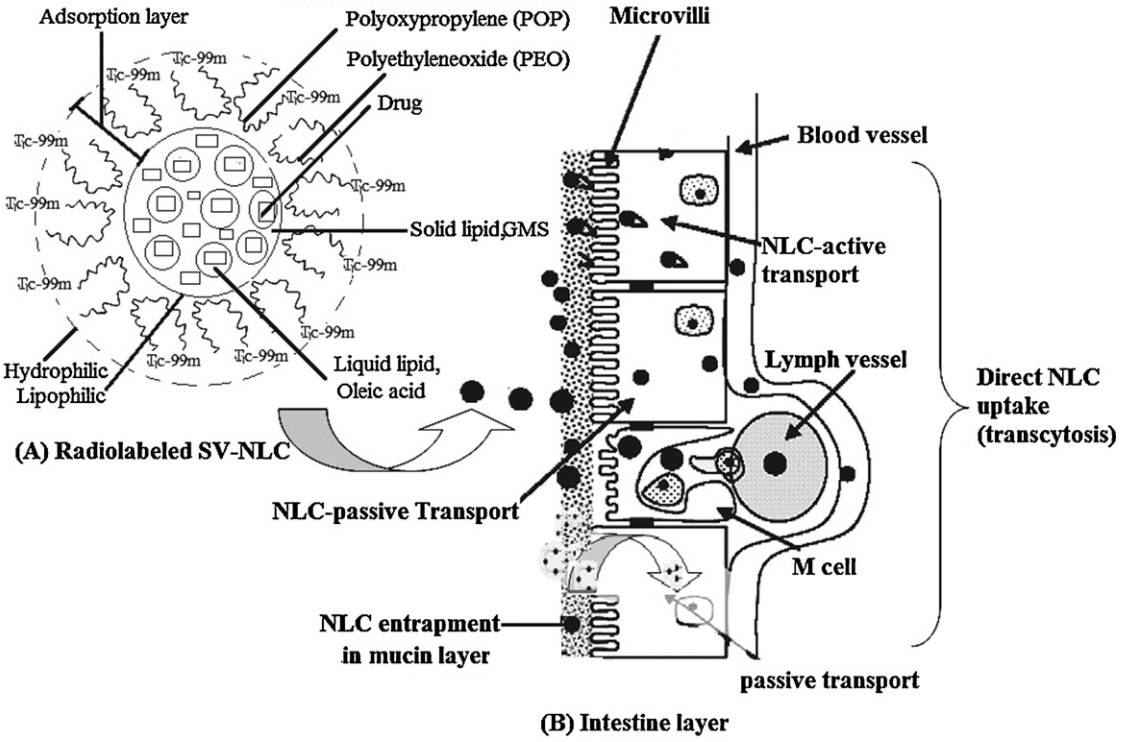

Fig. 10. Diagrammatic representation of the proposed absorption mechanisms of radiolabeled SV NLC.

diet and induce the bile secretion in small intestine, and mixed with the bile to form mixed micelles. These micelles can enhance the luminal solubility of the lipid digestion products, and also facilitate their passage across the unstirred water layer thereby providing a concentration gradient for absorption (Tso, 1994; Porter and Charman, 2001). Additionally, the presence of a region of low pH, adjacent to the enterocyte surface may provoke a change to the colloidal structure of the micellar species, presenting the intact NLCs available for lymphatic uptake (Jacobs et al., 2001). The uptake and lymphatic transport of intact colloidal nanosized NLCs supposedly played a dominant role in promoting absorption. A diagrammatic representation of the proposed absorption mechanism of SV NLC is presented in Fig. 10.

Predominantly, three mechanisms have been documented for the absorption of the NLC from the intestine that include direct uptake through the GI tract, increase in permeability by surfactants and decreased degradation and clearance. The particle size of the NLC formulations was almost less than 200 nm, and this reduced particle size improved the surface area of the NLCs. The fundamental equation used to support the design of nanoparticles systems is the equation of Ostwald–Freundlich which establishes the increase in solubility of a given substance on basis of the increase of interfacial energy at high curvatures of small sized particle (Kipp, 2004). This small size allows the efficient uptake in the intestine particularly in the lymphoidal section of the tissue thus by passing the first pass metabolism. Another factor that supports absorption of NLCs in the intestinal milieu, is the high dispersibility of NLCs. Besides this, the NLCs can also adhere on to the gut wall prolonging the residence time, and consequently the absorption. The presence of poloxamer 407 used as surfactant in formulation also supports the absorption of NLCs, due to its effect on intestinal epithelial permeability. Poloxamer is documented to deform the cell membrane and open the tight junction of the intestinal epithelial cell facilitating paracellular transport of NLCs (Wu and Lee, 2009). Poloxamer 407 also restrains p-glycoprotein efflux pump and increases NLC transport across the intestinal mucosa (Luo et al., 2006). Recently, it has been reported that enzyme activity of CYP3A could be inhibited by oleic acid (Mountfield et al., 2000). Thus it can be concluded that significant difference between the bioavailabilities of SV-NLC and SLNs was mainly due to the small particle size of NLC and presence of oleic acid in NLC.

Biodistribution studies indicated longer duration of radioactivity in the intestine that is attributable to higher amount of villi present in the intestine, in which nanoparticles can be easily entrapped for long period of time. Biodistribution of particulate drug carriers is greatly influenced by their size, surface characteristics and opsonization process. As a well known fact opsonins get adsorbed on the nanoparticle surface and promote particle recognition by RES organs. In our study NLCs showed higher accumulation in liver than suspension but the extent and pattern of biodistribution was similar for both the formulations, in spleen. Preferential uptake of NLCs by liver can be correlated to smaller size of particles and lymphatic uptake of lipid nanoparticles whereas the presence of charge on the surface of NLCs did not facilitate efficient coating with the opsonizing complement system resulting in reduced uptake by spleen (Manjunath and Venkateswarlu, 2005).

Interestingly the transport of NLCs through the intestinal lymphatic via the thoracic lymph duct to the systemic circulation at the junction of the jugular and left subclavian vein, bypasses the liver. SV is considered to be a reasonable substrate for intestinal lymphatic transport because of its high log p value. As evident from biodistribution studies that SV-NLCs continuously entered to liver even after 24 h of administration. This is attributed to the long circulatory time of SV-NLCs in blood. The long circulatory

Table 4
Percent uptake per gram organ weight (%A/G) following oral administration of radiolabeled SV suspension and SV-NLC in different organs of Balb/C mice.

Organs	%A/G at different organs at different time points									
	SV suspension					SV-NLC				
	1 h	2 h	4 h	24 h	48 h	1 h	2 h	4 h	24 h	48 h
Heart	0.001 ± 0.007*	0.2 ± 0.016*	0.01 ± 0.02*	0.009 ± 0.001	0.004 ± 0.001	0.01 ± 0.001	0.02 ± 0.1	0.006 ± 0.001	0.005 ± 0.001	0.002 ± 0.001
Lungs	0.013 ± 0.001	0.11 ± 0.03*	0.04 ± 0.03*	0.007 ± 0.001	0.003 ± 0.001	0.03 ± 0.003	0.06 ± 0.017	0.007 ± 0.002	0.004 ± 0.001	0.002 ± 0.001
Liver	0.009 ± 0.002*	0.06 ± 0.01*	0.06 ± 0.01*	0.04 ± 0.008*	0.032 ± 0.05*	0.04 ± 0.005	0.09 ± 0.01	0.36 ± 0.08	0.73 ± 0.14	0.11 ± 0.02
Spleen	0.039 ± 0.005	0.03 ± 0.006	0.04 ± 0.01	0.001 ± 0.002	0.001 ± 0.001	0.02 ± 0.01	0.03 ± 0.007	0.01 ± 0.001	0.004 ± 0.001	0.002 ± 0.001
Kidney	0.003 ± 0.001*	0.06 ± 0.01	0.05 ± 0.015	0.04 ± 0.01	0.02 ± 0.013	0.06 ± 0.015	0.07 ± 0.02	0.04 ± 0.01	0.04 ± 0.012	0.02 ± 0.01
Stomach	16.51 ± 1.32	14.75 ± 1.8	13.6 ± 1.86*	1.1 ± 0.02*	0.09 ± 0.027	16.96 ± 1.51	11.5 ± 2.03	9.08 ± 1.9	0.8 ± 0.13	0.014 ± 0.06
Intestine	3.3 ± 0.62*	1.35 ± 0.72*	0.9 ± 0.25*	0.04 ± 0.006*	0.02 ± 0.005	11.9 ± 1.86	18.36 ± 1.48	19.3 ± 3.12	3.6 ± 0.73	0.012 ± 0.01
Blood	0.01 ± 0.007	0.09 ± 0.02	0.05 ± 0.01	0.005 ± 0.001	0.0002 ± 0.001	0.03 ± 0.006	0.07 ± 0.016	0.16 ± 0.04	0.08 ± 0.016	0.01 ± 0.001

The p value for each organ is an unpaired t-test comparison between SV suspension and SV-NLC suspension oral delivery [$^*p < 0.05$].

time of SV-NLC in blood is credited to the stabilization of NLCs suspension, that was probably achieved by the addition of a surfactant poloxamer 407. During formation of NLCs, poloxamer gets adsorbed on the hydrophobic surface of NLCs via their hydrophobic polyoxypropylene center-block, and hydrophilic poloyoxyethylene side chain extend towards outside from NLCs surface. This type of arrangement provides a thermodynamically stable system in suspension by repulsion effect through a steric stabilization mechanism. Hydrophobic center block of poloxamer adheres on cell membrane and is capable of altering the biodistribution profile of NLCs. The hydrophilic poloyoxyethylene tails of poloxamer prevents the interaction between an approaching particles and the cells, and sticking of lipid nanoparticles to the blood vessel endothelium. This also suggests their phagocytic resistance and explains the long circulatory time of NLCs in the blood (Mohigimi et al., 2001). Long circulatory time of drug in the blood offered more partitioning of drug to the tissues resulting in higher organ uptake.

5. Conclusion

Simvasatin NLC suspension successfully optimized to achieve higher and sustained release as well as bioavailability of simvastatin. The obtained NLC was suspension of nanosized homogeneous particles with high entrapment efficiency and low recrystallization properties. The pharmacokinetic study demonstrated a higher relative bioavailability than both SV suspension and the SLN formulation that was directly a function of the presence of oily lipid in the NLC. The NLCs could improve the gastrointestinal absorption of SV and level A correlation could be established between *in vitro* dissolution and *in vivo* absorption. This work facilitates the use of nanostructured lipid carrier as a novel delivery system to enhance oral bioavailability of simvastatin.

Acknowledgments

Financial support was provided by All India Council for Technical Education (AICTE), New Delhi, India. Authors are grateful to Punjab University, Chandigarh, India, for providing TEM facility; IIT, Delhi, India, for providing assistance in DSC scan; CDRI, Lucknow, India, for providing zeta sizing facility.

References

Aungst, B.J., 2000. Intestinal permeation enhancers. J. Pharm. Sci. 89, 429–442.
Bolton, S., Bon, C., 2004. Pharmaceutical Statistics: Practical and Clinical Applications, 4th ed. Marcel Dekker, Inc., New York.
Christains, U., Jacobson, W., Floren, L.C., 1998. Metabolism and drug interactions of 3-hydroxy-3-methylglutaryl coenzyme A reductase inhibitors in transplant patients: are the statins mechanistically similar. Pharmacol. Ther. 80, 1–34.
Dixit, R.P., Nagarsenker, M.S., 2008. Formulation and in vivo evaluation of self-nanoemulsifying granules for oral delivery of a combination of ezetimibe and simvastatin. Drug Dev. Ind. Pharm. 34, 1285–1296.
Dressman, J.B., Reppas, C., 2000. In vitro–in vivo correlations for lipophilic, poorly water-soluble drugs. Eur. J. Pharm. Sci. 11, S73–S80.
Humberstone, A.J., Charman, W.N., 1997. Lipid based vehicles for the oral delivery of poorly water soluble drugs. Adv. Drug Deliv. Rev. 25, 103–128.
Jacobs, J., Kayser, O., Muller, R.H., 2001. Production and characterization of mucoadhesive nanosuspensions for the formulation of bupravaquone. Int. J. Pharm. 214, 3–7.
Kang, B.K., Lee, J.S., Chon, S.K., Joeng, S.Y., Yuk, S.K., Khang, G., Lee, H.B., Cho, S.H., 2004. Development of self-microemulsifying drug delivery systems for oral bioavailability enhancement of simvastatin in beagle dogs. Int. J. Pharm. 274, 65–73.
Kipp, J.E., 2004. The role of solid nanoparticle technology in the parenteral delivery of poorly water-soluble drugs. Int. J. Pharm. 284, 109–122.
Lai, J., Chen, J., Lu, Y., Sun, J., Hu, F., Yin, Z., Wu, W., 2009. Glyceryl monooleate/poloxamer 407 cubic nanoparticles as oral drug delivery systems. I. In vitro evaluation and enhanced oral bioavailability of the poorly water-soluble drug simvastatin. AAPS PharmSciTech 10, 960–966.
Li, H., Zhao, X., Ma, Y., Zhai, G., Li, L., Lou, H., 2009. Enhancement of gastrointestinal absorption of quercitin by solid lipid nanoparticles. J. Control. Release 133, 238–244.

Lilja, J.J., Neuvonen, M., Neuvonen, P.J., 2004. Effects of regular consumption of grapefruit juice on the pharmacokinetics of simvastatin. Br. J. Clin. Phramacol. 58, 56–60.

Luo, Y., Chen, D.W., Ren, L.X., Zhao, X.L., Qin, J., 2006. Solid lipid nanoparticles for enhancing vinpocetine's oral bioavailability. J. Control. Release 114, 53–59.

Mahley, R.W., Bersot, T.P., 2006. Drug therapy for hypercholesterolemia and dyslipidemia. In: Gilman, A.G., Goodman, L.S., Rall, T.W., Murad, F. (Eds.), The Pharmacological Basis of Therapeutics. , 11th ed. McGraw Hill Medical Publishing Div., New Delhi, pp. 933–966.

Manjunath, K., Venkateswarlu, V., 2005. Pharmacokinetics, tissue distribution and bioavailability of clozapine solid lipid nanoparticles after intravenous and intraduodenal administration. J. Control. Release 107, 215–228.

Mohamed, A.A.M., Sayed, H.K., Mohsen, A.B., Abdulaziz, A.A.A., 1998. Oral administration of liposomes containing cyclosporine: a pharmacokinetic study. Int. J. Pharm. 168, 163–168.

Mohigimi, S.M., Hunter, A.C., Murray, C., 2001. Long circulating and target specific nanoparticles: Theory and Practice. Pharmacol. Rev. 53, 283–318.

Mountfield, R.J., Senepin, S., Schleimer, M., Walter, L., Bittner, B., 2000. Potential inhibitory effects of formulations ingredients on intestinal cytochrome P450. Int. J. Pharm. 211, 89–92.

Muller, R.H., Mader, K., Gohla, S., 2000. Solid lipid nanoparticles for controlled drug delivery – a review of the state of the art. Eur. J. Pharm. Biopharm. 50, 161–177.

Paliwal, R., Rai, S., Vaidya, B., Khatri, K., Goyal, A.K., Mishra, N., Mehta, A., Vyas, S.P., 2009. Effect of lipid core material on characteristics of solid lipid nanoparticles designed for oral lymphatic delivery. Nanomedicine 5, 184–191.

Patil, P., Patil, V., Pardadhkar, A., 2007. Formulation of a self-emulsifying system for oral delivery of simvastatin: in vitro and in vivo evaluation. Acta Pharm. 57, 111–122.

Porter, C.J.H., Charman, W.N., 2001. Transport and absorption of drugs via lymphatic system. Adv. Drug Deliv. Rev. 50, 61–80.

Shah, M., Chuttani, K., Mishra, A.K., Pathak, K., 2010. Oral solid compitrol 888 ATO nanosuspension of simvastatin: optimization and biodistribution studies. Drug Dev. Ind. Pharm. 37, 526–537.

Shah, M., Pathak, K., 2010. Development and statistical optimization of solid lipid nanoparticles of simvastatin by using 2^3 full-factorial design. AAPS PharmSciTech 11, 489–496.

Silva, T.D., Areantes, V.T., Resende, J.A., Speziali, N.L., De Oliveira, R.B., Vianna-Soares, C.D., 2010. Preparation and characterization of solid dispersion of simvastatin. Drug Dev. Ind. Pharm. 36, 1348–1355.

Souto, E.B., Mehnert, W., Muller, R.H., 2006. Polymorphic behavior of Compritol 888 ATO as bulk lipid and as SLN and NLC. J. Microencapsul. 23, 417–433.

Suresh, G., Manjunath, K., Venkateswarlu, V., Satyanarayana, V., 2007. Preparation, characterization, and in vitro–in vivo evaluation of lovastatin solid lipid nanoparticles. AAPS PharmSciTech 8, E1–E9.

Tso, P., 1994. Intestinal lipid absorption. In: Johnson, L.R. (Ed.), Physiology of the Gastrointestinal Tract. Raven Press, New York, pp. 1867–1907.

Vishwanathan, A., 2008. A thesis on in vitro characterization of simvastatin loaded microspheres in the PolyRing device. 1–79.

Wu, G., Lee, K.Y.C., 2009. Effects of Poloxamer 188 on phospholipid monolayer morphology: an atomic force microscopy study. Langmuir 25, 2133–2139.

Zhuang, C., Li, N., Wang, M., Zhang, X., Pan, W., Peng, J., Pan, Y., Tang, X., 2010. Preparation and characterization of vinpocetine loaded nanostructured lipid carriers for improved oral bioavailability. Int. J. Pharm. 394, 179–185.